Geophys. J. R. astr. Soc. (1981) **67**, 791–799

Research note

Numerical evaluation of the Hilbert transform by the Fast Fourier Transform (FFT) technique

Hsi-Ping Liu *US Geological Survey, Menlo Park, California 94025, USA*
Dan D. Kosloff *Department of Geology, University of Houston, Houston, Texas 77004, USA*

Received 1981 March 27; in original form 1980 December 3

Summary. Three Fast Fourier Transform numerical methods for computing the Hilbert transform have been evaluated for their accuracy by numerical examples. All three methods employ the property that the Hilbert transform is a convolution. The first method uses the result that the Fourier transform of $1/\pi x$ is $-\mathrm{isgn}(\omega)$. The second method is based on a discrete Hilbert transform introduced by Saito. The third method, introduced in this research note, uses linear interpolation to transform the Hilbert transform integral into a discrete convolution. The last method is shown by numerical examples from fault dislocation models to be more accurate than the other two methods when the Hilbert transform integral has high-frequency components.

1 Introduction

The Hilbert transform appears frequently in geophysics. Some of the examples are:

(1) If the impulse response of a linear system is a causal real function of time, the real and imaginary parts of the transfer function form a Hilbert transform pair (Carlson 1968). The stress–strain relation for seismic wave propagation in the Earth's crust and mantle can be modelled by a linear anelastic solid with a distribution of relaxation times (Liu, Anderson & Kanamori 1976). The impulse response of such a linear anelastic solid is causal and real (Liu *et al.* 1976). The corresponding Hilbert transform pair is the Kramers–Krönig relation connecting phase velocity and attenuation,

$$\mathrm{Re}\{n(\omega)-n(\infty)\} = -\frac{1}{\pi} P \int_{-\infty}^{\infty} \frac{\mathrm{Im}\{n(u)\}}{\omega-u}\, du \tag{1}$$

$$\mathrm{Im}\{n(\omega)\} = \frac{1}{\pi} P \int_{-\infty}^{\infty} \frac{\mathrm{Re}\{n(u)\}}{\omega-u}\, du \tag{2}$$

$$n(\omega) = 1/v_p(\omega) + i\alpha(\omega)/\omega \tag{3}$$

where $v_p(\omega)$ is the phase velocity and $\alpha(\omega)$ the attenuation factor. The letter P before the integral sign denotes the Cauchy principal value. Futterman (1962) constructed several seismic wave absorption–dispersion pairs by analytically evaluating the Hilbert transform integral. (2) If the transfer function $F(\omega)$ of a causal system has no singularity in the complex lower half-plane, the logarithm of the amplitude response and the phase response from a Hilbert transform pair, i.e. if

$$F(\omega) = A(\omega) \exp [i\Phi(\omega)] \tag{4}$$

then

$$\ln A(\omega) = \frac{1}{\pi} P \int_{-\infty}^{\infty} \frac{\Phi(u)}{\omega - u} du \tag{5}$$

$$\Phi(\omega) = -\frac{1}{\pi} P \int_{-\infty}^{\infty} \frac{\ln A(u)}{\omega - u} du. \tag{6}$$

The class of functions with this property is called minimum-phase-shift (Papoulis 1962). Bolduc, Ellis & Russell (1972) determined the phase response of a minimum-phase-shift seismic system directly from the amplitude response by the Hilbert transform. They evaluated the Hilbert transform integral numerically for each ω by Simpson's rule. (3) If the Fourier components of a function $f(t)$ are all advanced in phase by a constant amount, then the resulting function can be calculated from a linear combination of $f(t)$ and its Hilbert transform (Arons & Yennie 1950). This property can be applied in seismology to plane waves supercritically reflected or transmitted at discontinuous boundaries inside the Earth (Aki & Richards 1980). The Hilbert transform can therefore be used in the construction of synthetic seismograms. (4) Mathematically, the problem of quasi-static slip on a two-dimensional fault with a given frictional behaviour on the fault surface can be represented by movement of a continuous distribution of dislocations (Weertman 1967, 1979; Savage 1980). Let $\sigma_f(x, t, \delta, \dot{\delta})$ be the friction stress as a function of x, distance along the fault, t, time, δ, slip displacement, and $\dot{\delta} = \partial\delta/\partial t$, slip velocity. If slip takes place only on a finite segment of the fault, $c < x < d$, the fault slip problem is described by the following equations,

$$\sigma_0(x, t) + \sigma_1(x, t) = \sigma_f(x, t, \delta, \dot{\delta}) \tag{7}$$

and

$$\sigma_1(x, t) = \frac{\mu}{2\pi\alpha} P \int_c^d \frac{\partial\delta(\xi, t)/\partial\xi}{x - \xi} d\xi \tag{8}$$

with the auxiliary condition

$$\int_c^d \frac{\sigma_1(x, t)}{(d-x)^{1/2}(x-c)^{1/2}} dx = 0 \tag{9}$$

where $\sigma_0(x, t)$ is the tectonic shear stress, $\sigma_1(x, t)$ the internal shear stress as a result of slip on the fault, μ the shear modulus, and under plane strain conditions $\alpha = 1 - \nu$, where ν is Poisson's ratio if δ is in the x-direction (edge-dislocation) and $\alpha = 1$ if δ is in the direction perpendicular to x and in the plane of the fault (screw dislocation). Equation (8) expresses the internal shear stress $\sigma_1(x, t)$ in terms of the finite Hilbert transform of the Burgers-vector density $\partial\delta(x, t)/\partial x$. Weertman (1979) solved analytically two examples of fault slip with a step function friction stress $\sigma_f(\dot{\delta})$ which depends only on the slip velocity $\dot{\delta}$. Numerical schemes of solution for the fault problem equations (7)–(9) are required in general for more realistic fault friction behaviour.

2 Numerical evaluation of the Hilbert transform by the Fast Fourier Transform (FFT) technique

2.1 TWO EXISTING FORMULAE

Let $f(x)$ be the Hilbert transform of the function $g(x)$,

$$f(x) = \frac{1}{\pi} P \int_{-\infty}^{\infty} \frac{g(\xi)}{x - \xi} \, d\xi. \tag{10}$$

Equation (10) shows $f(x)$ is a convolution of $g(x)$ and $1/\pi x$. By the convolution theorem of Fourier transform

$$F(\omega) = -\text{isgn}(\omega) \cdot G(\omega) \tag{11}$$

where $F(\omega)$ and $G(\omega)$ are the Fourier transforms of $f(x)$ and $g(x)$ respectively and $-\text{isgn}(\omega)$ is the Fourier transform of the function $1/\pi x$ (Bracewell 1978), i.e.

$$\lim_{\epsilon \to 0} \left(\int_{-\infty}^{-\epsilon} + \int_{\epsilon}^{\infty} \right) \frac{\exp(-i2\pi\omega x)}{\pi x} \, dx = -\text{isgn}(\omega). \tag{12}$$

Equation (11) suggests one method of evaluation of the Hilbert transform (10).

Method 1. Evaluate first the FFT of the function $g(x)$ to obtain $G_{\text{FFT}}(\omega)$. Multiply $G_{\text{FFT}}(\omega)$ by $-\text{isgn}(\omega)$. Finally, evaluate the inverse FFT of $-\text{isgn}(\omega) \cdot G_{\text{FFT}}(\omega)$ which yields an approximation to the Hilbert transform (10).

Saito (1974) introduced a discrete Hilbert transform for sampled functions which conserve all the important properties of the Hilbert transform (10). In correspondence to equation (10), this discrete Hilbert transform can be written as

$$f(x) = f(n \cdot \Delta x) = \frac{1}{\pi} {\sum_{m}}' \, g(m \cdot \Delta x) \frac{1 - \cos \pi (n - m)}{(n - m)\Delta x} \tag{13}$$

$$m, n = 0, \pm 1, \pm 2, \pm 3, \ldots, \pm\left(\frac{N}{2} - 1\right), \frac{N}{2}$$

where N is a power of 2 and the prime on the summation sign indicates the singular term when $n = m$ is to be omitted. In the limit $N \to \infty$, $\Delta x \to 0$, and $N\Delta x \to \infty$, equation (13) reduces to the conventional Hilbert transform. Saito's formula (13) suggests another method of evaluating equation (10) numerically.

Method 2 (Saito's method). First perform the FFT on $g(x)$ and on $(1\text{-}\cos(\pi x/\Delta x))/\pi x$ sampled at $x = m \cdot \Delta x$. Multiply the resulting FFTs to obtain $F_{\text{FFT}}(\omega)$. Finally take the inverse FFT of $F_{\text{FFT}}(\omega)$ to obtain the discrete Hilbert transform.

Both methods 1 and 2 approach the correct answer to equation (10) in the limit $N \to \infty$, $\Delta x \to 0$ and $N \cdot \Delta x \to \infty$.

The relative accuracy of the two methods for given N and Δx can be compared with the following two numerical examples.

The first example is taken from the linear-friction model on a two-dimensional fault (Weertman 1964; Savage 1980). For the displacement

$$\delta(x) = \begin{cases} \dfrac{2k\alpha}{\pi\mu} \left\{ d(d^2 - x^2)^{1/2} - x^2 \ln \dfrac{d}{x} \left(+ \dfrac{(d^2 - x^2)^{1/2}}{x} \right) \right\}, & x^2 \leq d^2 \\ 0, & x^2 > d^2 \end{cases} \tag{14}$$

the internal shear stress $\sigma_1(x)$ is given by

$$\sigma_1(x) = \frac{\mu}{2\pi\alpha} P \int_{-\infty}^{\infty} \frac{d\delta(\xi)/d\xi}{x-\xi} d\xi.$$

This integral can be evaluated analytically to give

$$\sigma_1(x) = \begin{cases} kx - 2kd/\pi, & x^2 \leqslant d^2 \\ \dfrac{2k}{\pi\alpha}\left\{ x \sin^{-1}\left(\dfrac{d}{x}\right) - d \right\}, & x^2 > d^2. \end{cases} \tag{15}$$

Fig. 1 shows the differences, Δ, between the stress $\sigma_1(x)$ computed by the two FFT methods and the analytic result equation (15). The parameters are $d = 2$, $\mu = 2$, $k = 1$, $\Delta x = 0.01$ (arbitrary unit), $\alpha = 1$, and $N = 1024$. The agreement between the values computed by Saito's method and those given by the analytical result, equation (15), is better than 0.1 per cent in the range $-3 < x < 3$ except at the two points $x = \pm 2$ (error = 3.2 per cent) where the analytical expression equation (15) has discontinuous derivatives of all orders. On the other hand, the error of the values computed by method 1 is greater than 2.4 per cent except at the two points $x = \pm 2$ (error = 0.8 per cent). The reason the results computed by Saito's method (method 2) deviate from the analytical solution towards both ends of the sampled region is that the discrete Fourier transform of a sampled function is periodic with a period of $N \cdot \Delta x$. This 'wrap-around' effect is illustrated in Fig. 2. Caution must therefore be taken when using this method to solve the fault slip problem by restricting the slipping region to the middle portion of the sampled region. This can always be achieved by including extra lengths of non-slipping fault segments outside of the region of interest into the sampling interval. This numerical example shows that Saito's method (method 2) is superior to method 1 in approximating the Hilbert transform (equation 10).

The second example is taken from another fault dislocation model. Slip is confined in this case to $-d < x < d$ where the frictional stress is a given constant. The solution with a constant applied shear stress is given by

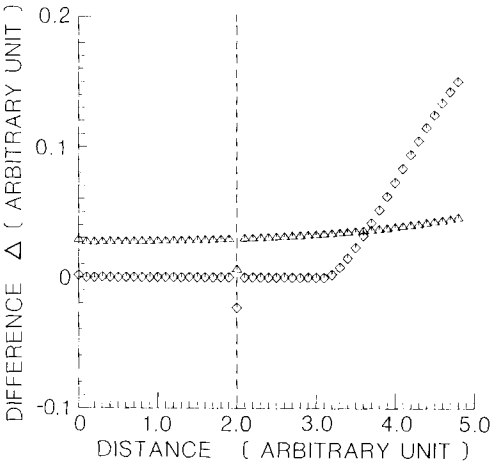

Figure 1. Difference, Δ, between the stress $\sigma_1(x)$ computed by two FFT methods and the analytical result of example 1 (linear-friction model on a two-dimensional fault). Triangular symbols: method 1. Diamond symbols: Saito's method (method 2). Dashed line indicates the position where the analytical expression equation (15) has discontinuous derivatives of all orders.

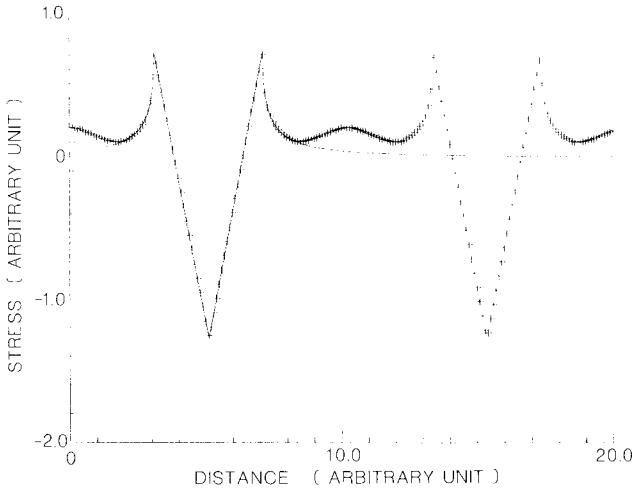

Figure 2. Showing the 'wrap-around' effect of FFT methods. Solid line, analytic results of stress as a function of distance in the linear-friction model on a two-dimensional fault. Crosses, results computed by Saito's method (method 2).

$$\delta(x) = \begin{cases} \dfrac{2\alpha}{\mu}\,(\sigma_t - \sigma_f)\,(d^2 - x^2)^{1/2}, & x^2 \leqslant d^2 \\ 0, & x^2 > d^2 \end{cases} \tag{16}$$

and

$$\sigma_1(x) = \frac{\mu}{2\pi\alpha}\, P \int_{-\infty}^{\infty} \frac{d\delta(\xi)/d\xi}{x-\xi}\, d\xi.$$

This integral can also be evaluated analytically to give

$$\sigma_1(x) = \begin{cases} \sigma_f - \sigma_t, & x^2 \leqslant d^2 \\ (\sigma_f - \sigma_t)\,\{1 - |x|/(x^2 - d^2)^{1/2}\}, & x^2 > d^2. \end{cases} \tag{17}$$

The internal shear stress $\sigma_1(x)$ is discontinuous and it has a singularity at $x = \pm d$ (Weertman 1964; Savage 1980). Fig. 3 shows the difference, Δ, between the stress calculated by FFT method 1 and the analytic result (equation 17). Fig. 4 is the corresponding figure for Saito's method (method 2). The parameters are $d = 2$, $\mu = 2$, $\Delta x = 0.01$, $\sigma_t - \sigma_f = 1$ (arbitrary units) $\alpha = 1$ and $N = 1024$. The FFT results computed by Saito's method (method 2) oscillate around the analytical result (17). The FFT results computed by method 1 oscillate mostly to one side of the analytical solution (17). These oscillations persist even away from the points of discontinuity $x = \pm 2$ where Gibbs' phenomenon of the Fourier methods is normally expected. These results indicate that both methods 1 and 2 are inadequate in approximating Hilbert transforms with high-frequency contents. We have devised a new FFT method to evaluate numerically the Hilbert transform which does not have this shortcoming.

2.2 A NEW METHOD

Let $x = m\Delta x$ where m is an integer and break the x-axis into intervals of size Δx. The Hilbert transform integral (10) is now given by

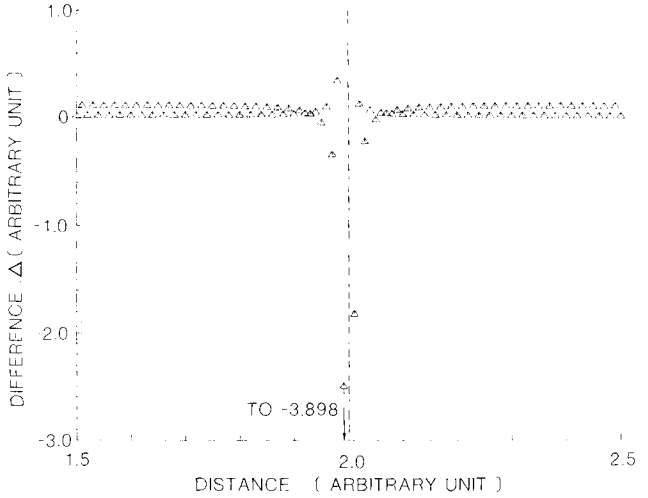

Figure 3. Difference, Δ, between the stress $\sigma_1(x)$ computed by FFT method 1 and the analytical result of example 2 (confined slip on a two-dimensional, constant-friction fault). The oscillations of Δ persist away from the point of discontinuity at $x = 2$ as indicated by the dotted line.

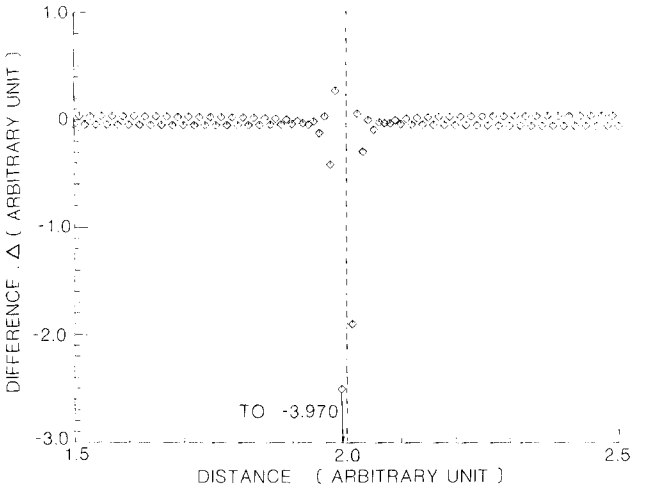

Figure 4. Difference, Δ, between the stress $\sigma_1(x)$ computed by Saito's method (method 2) and the analytical result of example 2 (confined slip on a two-dimensional constant-friction fault). The oscillations of Δ persist away from the point of discontinuity at $x = 2$ as indicated by the dotted line.

$$I = \frac{1}{\pi} \sum_{n=-\infty}^{\infty} \int_{n\Delta x}^{(n+1)\Delta x} \frac{g(\xi)}{x-\xi}\, d\xi. \tag{18}$$

Consider the contribution to I from the $(n-1)$th and the nth intervals. Using linear interpolation,

$$g(x) = P_{n-1}(x)\, g_{n-1} + P_n(x)\, g_n \tag{19}$$

in the $(n-1)$th interval and

$$g(x) = P_n(x)\, g_n + P_{n+1}(x)\, g_n \tag{20}$$

in the nth interval, where g_{n-1}, g_n, and g_{n+1} are function values of $g(x)$ at $x = (n-1)\Delta x$, $n\Delta x$ and $(n+1)\Delta x$ respectively and the interpolation function $P_n(x)$ is given by

$$P_n(x) = \begin{cases} \dfrac{x-(n-1)\Delta x}{\Delta x}, & (n-1)\Delta x \leqslant x \leqslant n\Delta x \\ \dfrac{(n+1)\Delta x - x}{\Delta x}, & n\Delta x \leqslant x \leqslant (n+1)\Delta x \\ 0, & x < (n-1)\Delta x \text{ or } x > (n+1)\Delta x. \end{cases} \tag{21}$$

Denote the contribution to I containing g_n by I_n. Substituting equations (19) and (20) into equation (18),

$$I_n = \frac{1}{\pi}\int_{(n-1)\Delta x}^{n\Delta x} \frac{\{\xi-(n-1)\Delta x\}g_n}{(x-\xi)\Delta x}\,d\xi + \frac{1}{\pi}\int_{n\Delta x}^{(n+1)\Delta x} \frac{\{(n+1)\Delta x-\xi\}g_n}{(x-\xi)\Delta x}\,d\xi. \tag{22}$$

With $x = m\Delta x$, equation (22) is integrated to yield

$$I_n = \frac{g_n}{\pi}\left\{(n-m-1)\ln\left(\frac{m-n}{m-n+1}\right) + (m-n-1)\ln\left(\frac{n+1-m}{n-m}\right)\right\}, \quad m \neq n. \tag{23}$$

Therefore

$$I = \sum_{n=-\infty}^{\infty} h_{m-n}\, g_n/\pi \tag{24}$$

which is a discrete convolution where

$$h_n = \begin{cases} -(n+1)\ln\left(\dfrac{n}{n+1}\right) + (n-1)\ln\left(\dfrac{n-1}{n}\right), & n \neq 0 \\ 0, & n = 0. \end{cases} \tag{25}$$

h_0 is set to zero because the Hilbert transform integral (10) is a Cauchy principal value integral. The first few values of the sequence $\{h_n\}$ are $h_1 = 1.38629, h_2 = 0.52325, h_3 = 0.33980$, $h_4 = 0.25267$, $h_5 = 0.20136, \ldots$. It can be shown from equation (25) that $h_n \to 1/n$ as $n \to \infty$. A third method, method 3, to evaluate the Hilbert transform integral (10) numerically can be constructed from the discrete convolution formula equation (24).

Method 3 (Liu–Kosloff method or L–K method). Perform FFT on $g(x)$ sampled at $x = m\Delta x$ and on $\{h_n\}$. Multiply the resulting FFTs to obtain $F_{\mathrm{FFT}}(\omega)$. Finally take the inverse FFT of $F_{\mathrm{FFT}}(\omega)$ to obtain the discrete Hilbert transform.

The same two numerical examples used to test methods 1 and 2 have been applied to method 3. The agreement between the values computed by the L–K method (method 3) and the analytical expression equation (15) of example 1 is better than 0.1 per cent in the range $-3 < x < 3$ except at the two points $x = \pm 2$ (error = 4.97 per cent). This accuracy is the same as that obtained by Saito's method (method 2). Fig. 5 shows the difference, Δ, between the stress calculated by the L–K method (method 3) and the analytical expression equation (17) of example 2. The FFT results computed by the L–K method (method 3) oscillate around the analytical solution (17) only near the points of discontinuity at $x = \pm 2$ and converges rapidly to the analytical solution away from the points of discontinuity. Moreover, the successive oscillations near the points of discontinuity average to within 4 per

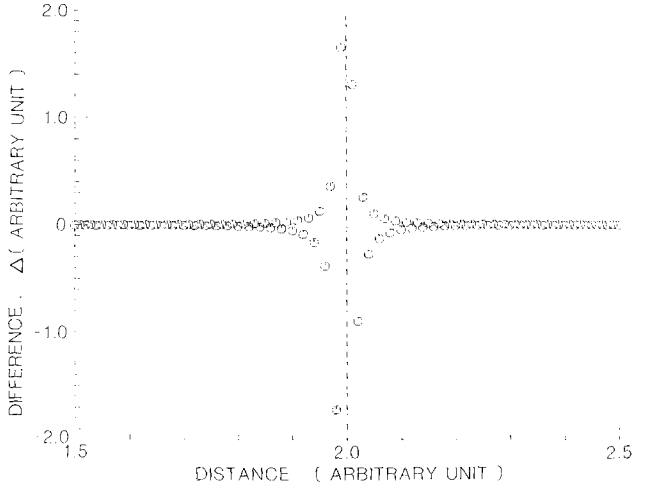

Figure 5. Difference, Δ, between the stress $\sigma_1(x)$ computed by the L–K method (method 3) and the analytical result of example 2 (confined slip on a two-dimensional, constant-friction fault). The oscillations of Δ diminish rapidly away from the point of discontinuity at $x = 2$ (indicated by the dashed line).

cent of the analytical solution. Such behaviour characterizes the Gibbs phenomenon which is common to all Fourier series and transform methods. In summary, the L–K method (method 3) is superior to both methods 1 and 2 because of its better approximation to Hilbert transform integrals whose spectra cover a wide frequency range.

3 Discussion

We have compared three FFT numerical methods which compute the Hilbert transform integral. The first method uses the result that the Fourier transform of $1/\pi x$ is $-\mathrm{isgn}(\omega)$. The second method (Saito's method) is based on a discrete Hilbert transform which in the limit of an infinite number of sampling points passes into the Hilbert transform integral (Saito 1974). Our devised third method uses linear interpolation to transform the Hilbert transform integral into a discrete convolution of the function values $\{g_n\}$ sampled at discrete points and another sequence $\{h_n\}$. The last method is shown by numerical example to be superior to the first two methods. We have not conducted a numerical analysis into the reason why the third method works the best. However, a few heuristic arguments can be offered. (1) Because the value of $1/\pi x$ decreases slowly with x, the FFT of $1/\pi x$ approaches $-\mathrm{isgn}(\omega)$ very slowly with an increase in the number of sampling points. This means that using the result that the Fourier transform integral of $1/\pi x$ is $-\mathrm{isgn}(\omega)$ in the FFT technique will cause some error. (2) The difference between Saito's (1974) method 2 and our method 3 is the same as that between the rectangle rule of grid interval $2\Delta x$ and trapezoid rule of grid interval Δx in numerical integration. The integrand $g(\xi)/(x-\xi)$ in equation (10) near the singularity $\xi = x$ is better approximated by the trapezoid rule (L–K method, method 3) than by the rectangle rule (Saito's method, method 2). Reducing the grid interval of Saito's method by a factor of 2 (thereby doubling the number of points used in the FFT) reduces the oscillation amplitude in Fig. 4 by ~ 25 per cent without changing its oscillatory behaviour.

Because of its capability to approximate accurately the Hilbert transform integrals with a wide frequency spectrum, method 3 has applications in solving quasi-static fault creep problems formulated by equations (7)–(9) when friction properties vary abruptly along the

fault (which implies a wide frequency spectrum in the stress solution) and when a large number of time steps are required to solve numerically the fault slip problem (which implies caution must be taken to reduce error accumulation during time stepping).

Acknowledgment

We thank J. C. Savage for useful discussions.

References

Aki, K. & Richards, P. G., 1980. *Quantitative Seismology, vol. 1,* W. H. Freeman, San Francisco.

Arons, A. B. & Yennie, D. R., 1950. Phase distortion of acoustic pulses obliquely reflected from a medium of higher sound velocity, *J. acoust. Soc. Am.,* **22,** 231–237.

Bolduc, P. M., Ellis, R. M. & Russell, R. D., 1972. Determination of the seismograph phase response from the amplitude response, *Bull. seism. Soc. Am.,* **62,** 1665–1672.

Bracewell, R. N., 1978. *The Fourier Transform and its Applications,* McGraw-Hill, New York.

Carlson, A. B., 1968. *Communication Systems, an Introduction to Signals and Noise in Electrical Communication,* McGraw-Hill, New York.

Futterman, W. I., 1962. Dispersive body waves, *J. geophys. Res.,* **67,** 5279–5291.

Liu, H.-P., Anderson, D. L., & Kanamori, H., 1976. Velocity dispersion due to anelasticity; implications for seismology and mantle composition, *Geophys. J. R. astr. Soc.,* **47,** 41–58.

Papoulis, A., 1962. *The Fourier Integral and its Applications,* McGraw-Hill, New York.

Saito, M., 1974. Hilbert transforms for sampled data, *J. Phys. Earth,* **22,** 313–324.

Savage, J. C., 1980. Dislocations in seismology, in *Dislocation Theory: a Treatise,* ed. Nabarro, F. R. N., North-Holland, Amsterdam.

Weertman, J., 1964. Continuum distribution of dislocations on faults with finite friction, *Bull. seism. Soc. Am.,* **54,** 1035–1058.

Weertman, J., 1967. Theory of infinitesimal dislocations distributed on a plane applied to discontinuous yield phemonena, *Can. J. Phys.,* **45,** 797–807.

Weertman, J., 1979. Inherent instability of quasi-static creep slippage on a fault, *J. geophys. Res.,* **84,** 2146–2152.